Transient statistics for two-mode gas ring lasers

A. Valle
Departamento de Física Moderna, Universidad de Cantabria and Instituto de Estudios Avanzados en Física Moderna y Biología Molecular, Consejo Superior de Investigaciones Científicas–Universidad de Cantabria, Avenida Los Castros, E 39005 Santander, Spain
A. Mecozzi
Fondazione Ugo Bordoni, via B. Castiglione 59, 00142 Roma, Italy
L. Pesquera and M. A. Rodríguez
Departamento de Física Moderna, Universidad de Cantabria and Instituto de Estudios Avanzados en Física Moderna y Biología Molecular, Consejo Superior de Investigaciones Científicas–Universidad de Cantabria, Avenida Los Castros, E 39005 Santander, Spain
P. Spano
Fondazione Ugo Bordoni, via B. Castiglione 59, 00142 Roma, Italy
(Received 12 January 1993)

Transient statistics that occur during the Q switching of two-mode gas ring lasers are studied, including the nonlinear regime. When both modes are well above threshold, explicit expressions for the transient intensity probability densities are obtained with the use of a quasideterministic theory. For similar pump parameters of the two modes, the intensity probability density of the secondary mode shows a polynomial tail due to mode competition. The main mode shows a symmetric tail and the probability density of the total intensity is peaked around its mean value (mode-partition noise). The anomalous fluctuations of the two modes are characterized by the maximum value of the variance of the intensity and by the time at which this maximum appears. We also consider the case of a very depressed secondary mode. An approximation is developed to describe the transient regime of the secondary mode. The transient probability densities and the side-mode excitation probability are obtained.

PACS number(s): 42.50.Ar, 42.60.Mi, 05.40.+j

I. INTRODUCTION

The statistics of laser switch-on has been recently considered in a variety of systems and situations (see Ref. [1] for a recent review). There are in general two different statistical problems to be studied. One is the statistics of the switch-on time at which laser emission is observed. This is described by the method of passage times (PT) in the linear regime of laser amplification. The second problem refers to the large statistical fluctuations of the laser intensity during a later nonlinear regime. For type-A lasers, results for PT statistics are well established [2], including the cases with pump noise (dye lasers) [3,4] and sweeping of the pump parameter [5, 6]. The problem of PT statistics for type-B lasers has also been considered for CO_2 [7] and semiconductor lasers [8, 9]. The intensity fluctuations in the nonlinear regime were considered for type-A lasers earlier [10, 11] than the PT statistics. More recent analysis includes the cases with pump noise [4], sweeping [12], and type-B lasers (semiconductor) [13, 14]. A description of the fluctuations in the nonlinear regime is possible by taking a simple average over a distribution of random initial values of the laser field. This is the basic idea of the quasideterministic theory (QDT) [15]. Most of the analysis of the laser switch-on problem considers the single-mode case. The transient multimode dynamics has been analyzed only in the linear regime for semiconductor [9, 16] and gas ring lasers [16].

In this paper we study transient statistics during the Q switching of two-mode on-resonance gas ring lasers, including the nonlinear regime. When the pump parameters of both modes, α_1 and α_2, are large with respect to the spontaneous-emission noise, we show that the transient regime can be described by the quasideterministic theory (QDT). This case corresponds to situations well above threshold. In the QDT the effect of the noise is replaced by an effective random initial condition, and the evolution in the nonlinear regime is deterministic. In this way explicit expressions for the transient intensity probability densities for both modes are obtained. In the case of nonequivalent modes, intensity fluctuations show a maximum. This is similar to the anomalous fluctuation peak found for a single-mode class-A laser.

When the pump parameters are slightly different, the intensity probability density for the secondary mode is shown to have a polynomial tail. This tail appears at times of order $(\alpha_1 - \alpha_2)^{-1}$. This time scale can be much larger than the time scales α_1^{-1} and α_2^{-1} corresponding to both modes. The main mode shows a symmetric tail. This tail corresponds to mode competition. In fact the probability density for the total intensity is peaked around its mean value. This phenomenon is similar to the mode-partition noise found in semiconductor lasers [17]. The anomalous intensity fluctuations of the two modes are characterized by the time at which the maximum of the variance of the intensity appears and by the value of this maximum. All these results are checked with numerical simulations.

We also consider the case of a very depressed secondary mode. Now the evolution of this mode is dominated by the noise. Then the QDT is not able to describe the transient regime of the secondary mode. We develop an approximation that includes the spontaneous-emission noise and a random pump parameter given by the intensity of the main mode, which is described by the QDT. Numerical simulations show that this approximation describes correctly the transient probability density for both modes and the side-mode excitation probability.

II. QUASIDETERMINISTIC THEORY (QDT)

The two-mode on-resonance gas ring laser can be described by the following equations [18]:

$$\dot{E}_1 = \frac{1}{2}\left[\alpha_1 - \beta(|E_1|^2 + |E_2|^2)\right]E_1 + \xi_1,$$
$$\dot{E}_2 = \frac{1}{2}\left[\alpha_2 - \beta(|E_1|^2 + |E_2|^2)\right]E_2 + \xi_2\,, \tag{2.1}$$

where $E_1(t)$ and $E_2(t)$ are the complex amplitudes of both modes, α_1 and α_2 are the pump parameters, and β is a constant. The complex random terms $\xi_1(t)$ and $\xi_2(t)$ model the spontaneous-emission noise. They are taken as Gaussian white noise of zero mean and correlation:

$$\langle \xi_i(t)\xi_j^*(t')\rangle = D\,\delta_{ij}\,\delta(t-t'), \quad i,j = 1,2\,. \tag{2.2}$$

We consider that the laser is initially below threshold and that at time $t = 0$ the laser is instantaneously switched on. We can easily obtain from Eq. (2.1) the intensity $I_i = |E_i|^2$, when saturation effects are negligible:

$$I_i(t) = |h_i(t)|^2\, e^{\alpha_i t}\,, \tag{2.3}$$

where $h_i(t)$ is a complex Gaussian process playing the role of an effective random initial condition for the deterministic evolution. The variance of this process is

$$\langle |h_i(t)|^2\rangle = \frac{D}{\alpha_i}(1 - e^{-\alpha_i t})\,. \tag{2.4}$$

The QDT [15] consists in approximating the actual process (2.1) by a process obtained from the nonlinear deterministic solution of (2.1), changing the initial condition by $|h_i(t)|^2$

$$I_i(t) = \frac{|h_i(t)|^2\, e^{\alpha_i t}}{1 + \beta\left[|h_1(t)|^2\,(e^{\alpha_1 t} - 1)/\alpha_1 + |h_2(t)|^2\,(e^{\alpha_2 t} - 1)/\alpha_2\right]}\,. \tag{2.5}$$

This approximation is valid whenever two different stages of evolution can be distinguished: an initial linear fluctuating regime and a nonlinear regime where the evolution is essentially deterministic. These different stages appear when the pump parameters are large with respect to the spontaneous-emission noise. For times such that $\exp(-\alpha_i t) \ll 1$, the effective initial condition $|h_i(t)|^2$ becomes a time-independent random variable. As a consequence, the evolution will be deterministic with a random initial condition. When the pump parameters are different, the steady state obtained from Eq. (2.5) is deterministic. Then the QDT can describe the fluctuations only during the transient regime.

The joint probability density $P(I_1, I_2; t)$ can be obtained from Eq. (2.5):

$$P(I_1, I_2; t) = \frac{1}{a_1(t)a_2(t)f(I_1, I_2, t)^3} \times \exp\left[-\left(\frac{I_1}{a_1(t)} + \frac{I_2}{a_2(t)}\right)f(I_1, I_2, t)^{-1}\right], \tag{2.6}$$

where

$$f(I_1, I_2, t) = 1 - \frac{I_1}{c_1(t)} - \frac{I_2}{c_2(t)} \tag{2.7}$$

and

$$a_i(t) = \frac{D}{\alpha_i}(e^{\alpha_i t} - 1), \quad c_i(t) = \frac{\alpha_i}{\beta(1 - e^{-\alpha_i t})}\,. \tag{2.8}$$

The domain in which $P(I_1, I_2; t)$ is defined is given by $f(I_1, I_2, t) > 0$.

Initially when $\exp(-\alpha_i t) \approx 1$, the evolution is dominated by the spontaneous emission and the modes are not coupled, i.e., $P(I_1, I_2; t) \approx P_1(I_1, t)P_2(I_2, t)$. When $a_i(t) > c_i(t)$, the modes are coupled through the deterministic evolution. This happens for times such that

$$\epsilon_i(t) = \frac{\alpha_i^2}{\beta D}\exp[-\alpha_i t] \tag{2.9}$$

is smaller than 1. Finally, it is easy to see from Eq. (2.5) that for nonequivalent modes ($\alpha_1 > \alpha_2$), the stationary state is reached in a time scale such that

$$u(t) = \frac{\alpha_1^2}{\alpha_2^2}\exp[-(\alpha_1 - \alpha_2)t] \tag{2.10}$$

is a small quantity. In the case of equal pump parameters, the steady state is reached when the modes become coupled, i.e., $\epsilon_i(t) < 1$.

The transient probability density function of the intensity of both modes can be derived from Eq. (2.6):

$$P_1(I_1, t) = \frac{c_2 a_2\left(c_2 a_2^{-1} + I_1[a_1(1 - I_1/c_1)]^{-1} + 1\right)}{a_1\left[c_2(1 - I_1/c_1) + a_2 I_1/a_1\right]^2} \times \exp\left[-\frac{I_1}{a_1(1 - I_1/c_1)}\right], \quad I_1 < c_1, \tag{2.11a}$$

$$P_2(I_2,t) = \frac{c_1 a_1 \left(c_1 a_1^{-1} + I_2[a_2(1-I_2/c_2)]^{-1} + 1\right)}{a_2\left[c_1(1-I_2/c_2) + a_1 I_2/a_2\right]^2} \times \exp\left[-\frac{I_2}{a_2(1-I_2/c_2)}\right], \quad I_2 < c_2\,. \tag{2.11b}$$

Finally, we consider the total intensity $I = I_1 + I_2$. This magnitude is relevant to analyze the coupling of the modes during the transient. From Eq. (2.6), we obtain the probability density function of I ($\alpha_1 > \alpha_2$):

$$P(I,t) = \frac{c_1 c_2 C(I,t)^2}{a_1 a_2 (c_1 - c_2)} \left\{ \left(\frac{I}{a_1}(1 - I/c_1)^{-1} + \frac{(a_1 - a_2)c_1 c_2}{(c_1 - c_2)a_1 a_2} + 1 \right) \exp\left[-\frac{I}{a_1(1 - I/c_1)} \right] - \left(\frac{I}{a_2}(1 - I/c_2)^{-1} + \frac{(a_1 - a_2)c_1 c_2}{(c_1 - c_2)a_1 a_2} + 1 \right) \exp\left[-\frac{I}{a_2(1 - I/c_2)} \right] \right\} \tag{2.12a}$$

when $I < c_2(t)$ and

$$P(I,t) = \frac{c_1 c_2 C(I,t)^2}{a_1 a_2 (c_1 - c_2)} \left\{ \left(\frac{I}{a_1}(1 - I/c_1)^{-1} + \frac{(a_1 - a_2)c_1 c_2}{(c_1 - c_2)a_1 a_2} + 1 \right) \exp\left[-\frac{I}{a_1(1 - I/c_1)} \right] \right\} \tag{2.12b}$$

when $c_2(t) < I < c_1(t)$. In these expressions, $C(I,t)$ is given by

$$C(I,t) = \left[\frac{I}{a_1} + \frac{(a_1 - a_2)c_1 c_2}{(c_1 - c_2)a_1 a_2} \left(1 - \frac{I}{c_1} \right) \right]^{-1}. \tag{2.13}$$

We have checked with numerical simulations [19] of Eq. (2.1) the validity of the QDT. The QDT is found to give a good approximation in the transient regime (see Figs. 1 and 2) unless a very depressed mode is considered. In this case, $\alpha_1 \gg \alpha_2$, the evolution of the secondary mode is dominated by the noise and an alternative approximation is required (see Sec. IV). However, the main mode is always well described by the QDT.

III. TRANSIENT STATISTICS IN THE MODE COMPETITION CASE

We analyze in this section the transient statistics when the pump parameters for both modes are slightly different, i.e., when the parameter γ, defined as

$$\gamma = \frac{\alpha_1}{\alpha_2} - 1, \tag{3.1}$$

is a small quantity. As noted in Sec. II, a new time scale $(\alpha_1 - \alpha_2)^{-1}$ appears when $\alpha_1 > \alpha_2$, apart from the usual ones α_1^{-1} and α_2^{-1}. This time scale is related to the competition between both modes and it can be much slower than the first two when $\alpha_1 \approx \alpha_2$. This time $(\alpha_1 - \alpha_2)^{-1}$ is the characteristic time at which the modes approach the stationary state. It is also the typical time for the main mode to be switched on if the side mode has been initially excited.

When the modes are coupled, i.e., $\epsilon_i(t) \ll 1$, the probability densities for both modes (2.11) can be approximated by

$$P_1(x_1,t) = \frac{u(t)}{\left\{1 - x_1\left[1 - u(t)\right]\right\}^2}, \quad x_1 < 1 \tag{3.2a}$$

$$P_2(x_2,t) = \frac{u^{-1}(t)}{\left\{1 + x_2\left[u^{-1}(t) - 1\right]\right\}^2}, \quad x_2 < 1 \tag{3.2b}$$

except in a small region $x_i \approx 1$ with a negligible contribution to the probability, where the exponential term must be taken into account. In these expressions, we use

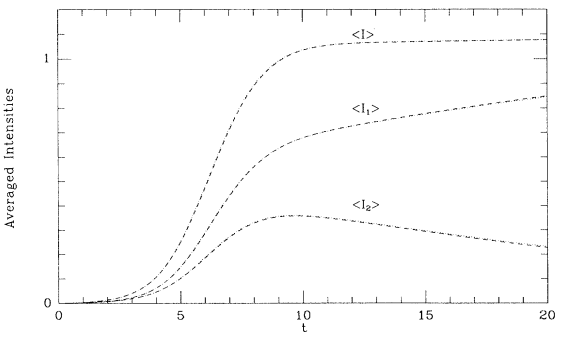

FIG. 1. Mean values of the main mode $\langle I_1 \rangle$, depressed mode $\langle I_2 \rangle$, and total $\langle I \rangle$ intensities. The simulation results are represented by the dotted line and the QDT by the dashed line. The parameters are taken as $\alpha_1 = 1.1$, $\alpha_2 = 1$, $\beta = 1$, and $D = 10^{-3}$.

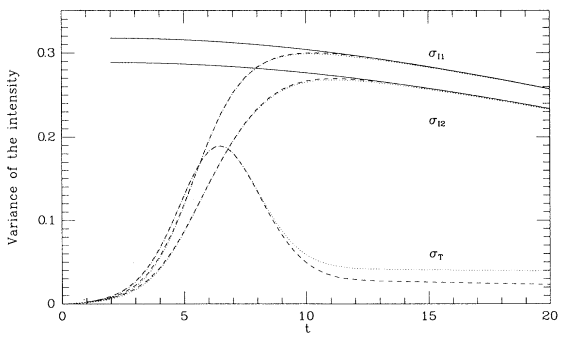

FIG. 2. Variances of the main mode σ_{I_1}, depressed mode σ_{I_2}, and total σ_T intensities. We also plot with the solid line the function given by Eq. (3.5). The parameters are the same as in Fig. 1.

the normalized modal intensities $x_i = \beta I_i/\alpha$. Note that $u(t) < 1$ when $\epsilon_i(t) < 1$. This is due to the fact that $\beta D/\alpha_1^2 \ll 1$, that is, the validity condition of the QDT. When $\epsilon_2(t) < 1$, we have $u(t) < (\gamma+1)^2(\beta D/\alpha_2^2)^\gamma$ that is always smaller than 1 for $\beta D/\alpha_2^2 < \exp(-2)$.

The probability density for the secondary mode has a polynomial tail and the main mode shows a symmetric tail for small values of the intensity (see Fig. 3). These distributions (3.2) are related in a simple way: the probability density of x_1 is given by that of $1 - x_2$. The tails correspond to mode competition. The tail for the main mode corresponds to realizations starting later with respect to most of the realizations. The meaning of the tail for the secondary mode is that, for those realizations for which the main mode starts later, there is a large probability that the secondary mode starts. For this reason, the dependence on x_2 of this tail is the same, but symmetric with respect to that of the main mode. In fact, at times such that $\epsilon_i(t) \ll 1$, the probability density for the total intensity is peaked around its mean value as in the mode-partition noise phenomenon found in semiconductor lasers [17] (see Fig. 3). Then, the variance of the total intensity σ_T is very small, in contrast with the variances of the two modes that take their maximum values when σ_T decreases. This behavior can be derived from Eq. (2.12), taking into account that for these times the exponential terms are equal to 1 when $I < (\alpha_2/\beta)$. Then the two terms in Eq. (2.12a) cancel each other and $P(I,t)$ is non-negligible only when the total intensity varies between (α_2/β) and (α_1/β).

The expressions for the probability densities given by Eqs. (3.2) show that when $\epsilon_i(t) \ll 1$, the temporal dependence of the normalized intensities $x_i(t)$ scales with $u(t)$. The mean intensity values are given by

$$\langle x_1(t)\rangle = 1 - \langle x_2(t)\rangle = \frac{1}{1-u} - \frac{u}{(1-u)^2}\ln u^{-1} . \quad (3.3)$$

Figure 4 shows the dynamical scaling given by $u(t)$.

We have also studied the scaling of the moments of the intensity of the secondary mode. We find from Eq. (3.2b) that for $n > 1$ and times such that $u(t) < 1$,

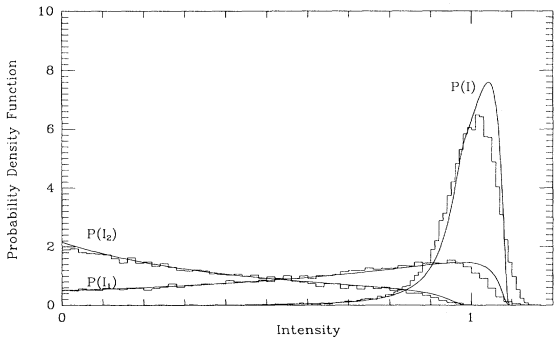

FIG. 3. Probability density function of the main mode, depressed mode, and total intensities at time $t = 9$. The simulation results are represented by the histogram and the QDT results by the solid curve. The parameters are the same as in Fig. 1.

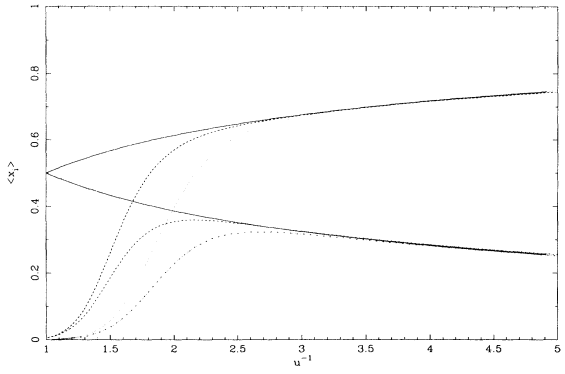

FIG. 4. Mean values obtained from simulation of the main-mode and depressed-mode normalized intensities as a function of u^{-1}. The mean values of the normalized main-mode intensity $\langle x_1\rangle$ are represented by the dashed line ($\alpha_2 = 1$) and the dotted line ($\alpha_2 = 3$), and the mean values of the normalized depressed-mode intensity $\langle x_2\rangle$ by the dot-dashed line ($\alpha_2 = 1$) and the three-dot-dashed line ($\alpha_2 = 3$). We also plot with the solid line the functions given by Eq. (3.3). Other parameters in the figure are $\gamma = 0.1$, $\beta = 1$, and $D = 10^{-3}$.

$$\langle x_2^n\rangle \approx \frac{u(t)}{n-1} . \quad (3.4)$$

This result shows the non-Gaussian character of the transient statistics.

We now study the transient fluctuations of the intensity using the QDT. When the modes are nonequivalent ($\alpha_1 > \alpha_2$), the intensity fluctuations of both modes show a maximum (see Fig. 2). This is similar to the anomalous fluctuation peak found for a single-mode class-A laser [10]. As concerns the total intensity $I = I_1 + I_2$, its variance also shows a maximum. We will characterize anomalous fluctuations of the two-mode normalized intensities by the time at which the maximum appears, $t_{m,i}$, and by the value of this maximum, $\sigma_{m,i}$. When $\epsilon_i(t) = [\alpha_i^2/(\beta D)]\exp[-\alpha_i t] \ll 1$, these fluctuations can be derived from Eq. (3.2):

$$\sigma_i^2(t) = \frac{u(t)}{[1-u(t)]^2} - \frac{u(t)^2}{[1-u(t)]^4}\left[\ln u(t)\right]^2 . \quad (3.5)$$

Then for these times the fluctuations of the normalized intensities coincide and they show a temporal dependence given by a dynamical scaling parameter $u(t)$ (see Fig. 5). This generalizes the dynamical scaling found in the single-mode case [20].

The variance given by Eq. (3.5) is a decreasing function of t in its validity region, given by $\epsilon_i(t) < 1$, and then $u(t) < 1$. Then it cannot be used to obtain the time at which the maximum of the fluctuations appears, $t_{m,i}$. The maximum appears when the modes become coupled, i.e., $\epsilon_i(t) \lesssim 1$ and the mode competition is strong. This corresponds to a time regime such that the mean intensity for the side mode takes its maximum value (see Figs. 1, 2, 4, and 5). For times such that side-mode intensity is depressed by the main mode, i.e., $\epsilon_i(t) \ll 1$, fluctuations decrease with time. When the pump parameters are sim-

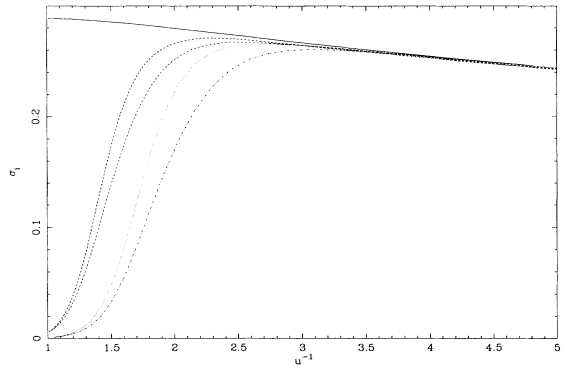

FIG. 5. Variances obtained from simulation of the main-mode and depressed-mode normalized intensities. The variance of the main-mode intensity σ_1 is represented by the dashed line ($\alpha_2 = 1$) and the dotted line ($\alpha_2 = 3$), and the variance of the depressed-mode intensity σ_2 by the dot-dashed line ($\alpha_2 = 1$) and the three-dot-dashed line ($\alpha_2 = 3$). We also plot with the solid line the function given by Eq. (3.5). The other parameters in the figure are the same as in Fig. 4.

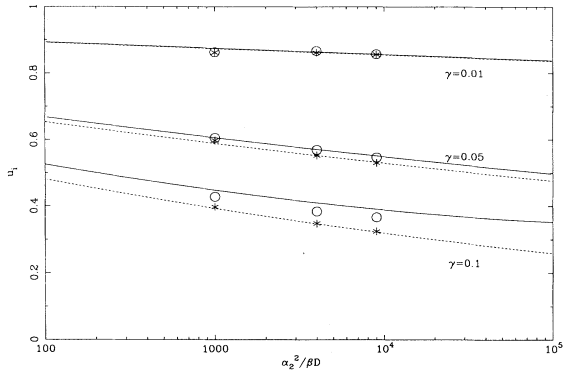

FIG. 6. u_1 and u_2 as functions of γ and $\alpha_2^2/(\beta D)$. The results given by Eqs. (3.6a) and (3.6b) are represented by the solid and dashed lines, respectively. The simulation results for u_1 are plotted with circles and for u_2 with stars. The parameters used in these simulations are $\alpha_2 = 1, 2, 3$, $\beta = 1$, and $D = 10^{-3}$.

ilar, i.e., γ is small, the competition between modes lasts for a long time and the variance changes very slowly (see Figs. 2 and 5). Then the variance obtained from Eq. (3.5) at $u = u(t_{m,i})$, that is valid when $\epsilon_i(t) \ll 1$, is a good approximation for $\sigma_{m,i}$ (see Figs. 2 and 5). However, since $\sigma_i(t)$ decreases for times $t < t_{m,i}$ in an appreciable way only when $\epsilon_i(t) \gtrsim 1$, Eq. (3.5) cannot describe this behavior.

To obtain $t_{m,i}$, we use Eqs. (2.11) instead of Eqs. (3.2). The main difference between these expressions lies in the exponential term. When γ is small, the moments for the mode intensities at $t_{m,i}$ can be obtained from Eqs. (3.2). Using this approximation, the following equations for $t_{m,i}$ can be derived:

$$g(u_1) = \left(\frac{\alpha_2^2}{\beta D}\right)\frac{u_1^{1/\gamma}}{(1+\gamma)^{2/\gamma}\gamma} \times\left[\frac{-1}{(1-u_1)} - \frac{2u_1}{(1-u_1)^3}\ln u_1^{-1} + \frac{2u_1}{(1-u_1)^4}(\ln u_1^{-1})^2 - \frac{\gamma}{u_1}\left(\frac{(1+u_1)}{(1-u_1)} - \frac{2u_1}{(1-u_1)^2}\ln u_1^{-1}\right)\right] \quad (3.6a)$$

$$g(u_2) = \left(\frac{\alpha_2^2}{\beta D}\right)\frac{u_2^{1/\gamma}}{(1+\gamma)^{2/\gamma}\gamma} \times\left[\frac{1}{(1-u_2)} - \frac{2u_2}{(1-u_2)^3}\ln u_2^{-1} + \frac{2u_2^2}{(1-u_2)^4}(\ln u_2^{-1})^2 - \gamma\left(\frac{(1+u_2)}{(1-u_2)} - \frac{2u_2}{(1-u_2)^2}\ln u_2^{-1}\right)\right], \quad (3.6b)$$

where

$$g(u) = \frac{(1+u)}{(1-u)^3} + \frac{2u}{(1-u)^4}\ln u^{-1} - \frac{2u(1+u)}{(1-u)^5}(\ln u^{-1})^2, \quad (3.7)$$

and $u_i = (\alpha_1/\alpha_2)^2 \exp[-(\alpha_1 - \alpha_2)t_{m,i}]$. In Fig. 6 it is shown that Eqs. (3.6) give correctly the time at which the maximum of the fluctuations appears and that the approximation works better when γ decreases.

It is not possible to get an analytic solution for u_i from Eq. (3.6). However, when γ decreases, u_i approaches 1 (see Fig. 6) and an approximation can be obtained. In this case, it is found that u_i changes very slowly with $(\alpha_2^2/\beta D)$ in the following way: $(1 - u_i) \approx \gamma \ln(\alpha_2^2/\beta D)$. Then u_i depends mainly on γ when the pump parameters are similar.

Finally we consider the case of equivalent modes, $\alpha_1 = \alpha_2 = \alpha$. Since the modes compete forever, the variance increases until the steady state is reached. Now the QDT describes the fluctuations in the stationary state [see Eq. (2.5)], which is given from Eq. (2.11) by an uniform probability between 0 and (α/β). This result is in agreement with the exact result [21] well above threshold.

IV. TRANSIENT STATISTICS IN THE VERY-DEPRESSED-MODE CASE

When the secondary mode is very depressed, $\alpha_2 \ll \alpha_1$, the evolution of I_2 is mainly due to the spontaneous-emission noise. Then the evolution is not deterministic and the QDT does not describe correctly the secondary mode. Since the effect of a very depressed secondary mode is negligible, the evolution of the main mode is given by the QDT for the single-mode laser:

$$I_1^{\mathrm{SM}}(t) = \frac{|\, h_1(\infty)\,|^2\, e^{\alpha_1 t}}{1 + (\beta/\alpha_1)\,|\, h_1(\infty)\,|^2\, e^{\alpha_1 t}}, \quad (4.1)$$

where we consider times such that $|\, h_1(t)\,|^2 \approx |\, h_1(\infty)\,|^2$,

that is, $e^{-\alpha_1 t} \ll 1$ [see Eq. (2.4)].

For the secondary mode, we develop an alternative approximation by using a random pump parameter given by the intensity of the main mode and by including the spontaneous-emission noise. Using this approximation, the evolution equation for the secondary mode is

$$\dot{E}_2 = \frac{1}{2}(\alpha_2 - \beta I_1^{\mathrm{SM}})E_2 + \xi_2 . \tag{4.2}$$

The probability density of I_2 can be obtained from the conditional probability density $P(I_2|I_1;t)$ by integrating over I_1 the function $P(I_1, I_2; t)$, defined by

$$P(I_1, I_2; t) = P(I_2 \,|\, I_1; t) P_1^{\mathrm{SM}}(I_1, t) . \tag{4.3}$$

In this expression, $P(I_2 \,|\, I_1; t)$ is an exponential distribution with mean value

$$\begin{aligned} \langle I_2 \,|\, I_1; t\rangle &= \frac{D}{\alpha_2}(e^{\alpha_2 t} - 1)\left(1 - \frac{\beta I_1}{\alpha_1}\right) + \frac{D}{\alpha_1}\frac{\beta I_1}{\alpha_1} \\ &\approx Dt\left(1 - \frac{\beta I_1}{\alpha_1}\right) + \frac{D}{\alpha_1}\frac{\beta I_1}{\alpha_1} , \end{aligned} \tag{4.4}$$

and $P_1^{\mathrm{SM}}(I_1, t)$ can be obtained from (4.1):

$$P_1^{\mathrm{SM}}(I_1, t) = \frac{\alpha_1 e^{-\alpha_1 t}}{D(1 - \beta I_1/\alpha_1)^2} \exp - \left[\frac{\alpha_1 e^{-\alpha_1 t} I_1}{D(1 - \beta I_1/\alpha_1)}\right] . \tag{4.5}$$

For short times such that $\epsilon_1(t) \gg 1$, the main-mode intensity is small and the side-mode intensity increases due to the spontaneous-emission noise. Then the probability density of I_2 is an exponential distribution with mean value Dt. For intermediate times such that $\alpha_1 t \epsilon_1 \gg 1$, the mean value (4.4) can be approximated by the first term and the following approximation holds:

$$P(I_2) = \frac{e^{-I_2/(Dt)}}{Dt}\left[\frac{1}{1 + I_2/(Dt\epsilon_1)} + \frac{1}{\epsilon_1\left[1 + I_2/(Dt\epsilon_1)\right]^2}\right] . \tag{4.6}$$

In this time regime, $\langle [I_2/(Dt)]^n \rangle$ is a function only of ϵ_1. Finally, when the steady state is attained, i.e., when $\epsilon_1(t) \ll 1$, the probability density of I_2 is again an exponential distribution with mean value D/α_1.

The moments of the intensity of the depressed mode can be easily obtained from Eqs. (4.4) and (4.5). The mean value is given by

$$\langle I_2(t)\rangle = \frac{D}{\alpha_1}\left[1 - \epsilon_1 e^{\epsilon_1} E_1(\epsilon_1)\right] + Dt\epsilon_1 e^{\epsilon_1} E_1(\epsilon_1) , \tag{4.7}$$

where E_1 is the exponential-integral function [22]. The fluctuations are given by

$$\sigma_2^2(t) = 2\left[\frac{D}{\alpha_1}(1 - \alpha_1 t)\frac{\beta\sigma_1(t)}{\alpha_1}\right]^2 + \langle I_2(t)\rangle^2 , \tag{4.8}$$

where σ_1 is the variance of the main mode:

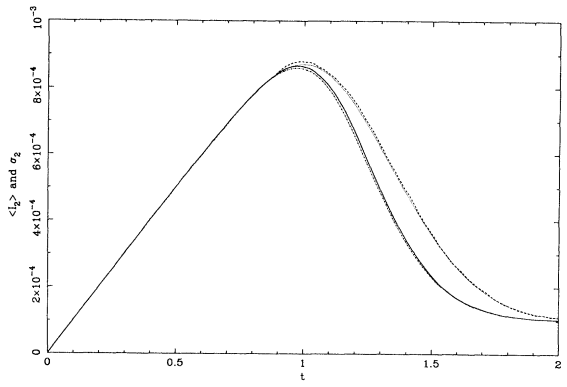

FIG. 7. Mean value and variance of the intensity of a very depressed mode. Simulation results for the mean value and the variance are represented by the solid and dashed lines, respectively. We also plot the mean value (dot-dashed line) and variance (dotted line) given by the approximation. The parameters in this figure are $\alpha_1 = 10$, $\alpha_2 = 0.01$, $\beta = 1$, and $D = 10^{-3}$.

$$\sigma_1(t)^2 = (\alpha_1/\beta)^2\left\{\epsilon_1 - \epsilon_1^2 e^{\epsilon_1} E_1(\epsilon_1)\left[e^{\epsilon_1} E_1(\epsilon_1) + 1\right]\right\} . \tag{4.9}$$

Figure 7 shows that the mean value and the variance of the depressed mode are well described by the approximation. We observe that initially $\langle I_2\rangle = \sigma_2 = Dt$, in agreement with the discussion above. When I_2 starts to be depressed by the main mode, we have $\langle I_2\rangle \approx \sigma_2 \approx Dt(1 - \langle \beta I_1/\alpha_1\rangle)$. This corresponds to small values of $\langle I_1\rangle$ and σ_1 [see Eqs. (4.4) and (4.7)–(4.9)]. This time regime, which includes the times at which the maximums of $\langle I_2\rangle$ and σ_2 appear, can be described by (4.6). When the main mode increases, the two terms in Eq. (4.4) are important and $\sigma_2 > \langle I_2\rangle$. Finally, in the steady state we have $\langle I_2\rangle = \sigma_2 = D/\alpha_1$.

Finally, we calculate the probability $\Phi(I_1)dI_1$ that

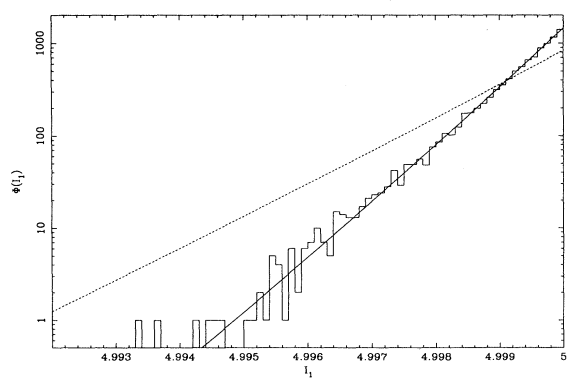

FIG. 8. $\Phi(I_1)$ obtained from simulation (histogram), linear theory (dashed line), and from (4.10) (solid line). The threshold intensity I_T has been fixed to one-half the stationary intensity of the main mode. The parameters are taken as $\alpha_1 = 10$, $\alpha_2 = 0.1$, $\beta = 1$, and $D = 10^{-3}$.

when the intensity is for the first time $I_1 + I_2 = I_T$, the main-mode intensity is between I_1 and $I_1 + dI_1$. This probability gives direct information about the side-mode excitation probability, and it has been obtained by neglecting the nonlinear terms for the semiconductor and gas lasers [16] when the side mode is not very depressed. The calculation of this probability is equivalent to finding, in the multidimensional phase space of the system, the direction of departure from the initial laser unstable point. The probability density $\Phi(I_1)$ can be written as a function of the probability current (J_1, J_2), associated to the Fokker-Planck equation equivalent to the Langevin equations of our approximation, in the following way:

$$\Phi(I_1) = \int_0^\infty (J_1 + J_2)(I_1, I_T - I_1)dt \ , \tag{4.10}$$

where

$$J_1(I_1, I_2, t) = (\alpha_1 - \beta I_1) I_1 P(I_1, I_2, t), \tag{4.11}$$

$$J_2(I_1, I_2, t) = (\alpha_2 - \beta I_1) I_2 P - D\left(I_2 \frac{\partial P}{\partial I_2} + P\right)(I_1, I_2, t) \ . \tag{4.12}$$

To obtain Φ, one should impose absorbing boundary conditions. However, a good approximation can be obtained by using natural boundary conditions. This corresponds to the fact that, for large enough values of α_1, the boundary $I_1 + I_2 = I_T$ is only crossed one time. In this way, we obtain that the function $P(I_1, I_2, t)$ appearing in the expression of the probability current coincides with (4.3). We compare in Fig. 8 $\Phi(I_1)$ calculated from (4.10) and by using the linear theory [16] with the simulation results. It is not possible to obtain an analytical expression for the integral appearing in (4.10). This integral is evaluated numerically by using (4.11), (4.12), and the joint probability density given by (4.3). It is clear that the approximation (4.10) gives very good results and that the linear theory is unable to describe correctly $\Phi(I_1)$.

ACKNOWLEDGMENTS

Financial support from DGICYT (Spain) Projects No. PS 90-0098 and No. TIC 90-080 is acknowledged. The activity performed at FUB was carried out under the agreement between the Fondazione Ugo Bordoni and the Italian PT Administration.

[1] M. San Miguel, in *Laser Noise*, edited by R. Roy (SPIE, Boston, 1990), p. 272.
[2] M. R. Youngh and S. Singh, Phys. Rev. A **35**, 1453 (1987); J. Opt. Soc. Am. B **5**, 1011 (1988).
[3] R. Roy, A. W. Yu, and S. Zhu, Phys. Rev. Lett. **55**, 2794 (1985); Phys. Rev. A **34**, 4333 (1986).
[4] F. De Pasquale, J. M. Sancho, M. San Miguel, and P. Tartaglia, Phys. Rev. Lett. **56**, 2473 (1986).
[5] G. Broggi, A. Colombo, L. A. Lugiato, and P. Mandel, Phys. Rev. A **33**, 3635 (1986).
[6] M. C. Torrent and M. San Miguel, Phys. Rev. A **35**, 1453 (1987).
[7] F. T. Arecchi, R. Meucci, and J. A. Roversi, Europhys. Lett. **8**, 225 (1989); F. T. Arecchi, W. Gadomsky, R. Meucci, and J. A. Roversi, Phys. Rev. A **39**, 4004 (1989); M. Ciofini, R. Meucci, and F. T. Arecchi, *ibid.* **42**, 482 (1990).
[8] A. Mecozzi, S. Piazzolla, A. D'Ottavi, and P. Spano, Phys. Rev. A **38**, 3136 (1988); Appl. Phys. Lett. **55**, 769 (1989).
[9] P. Spano, A. D'Ottavi, A. Mecozzi, B. Daino, and S. Piazzolla, IEEE J. Quantum Electron. **25**, 1440 (1989).
[10] F. T. Arecchi, V. de Giorgio, and B. Querzola, Phys. Rev. Lett. **19**, 1168 (1967); F. T. Arecchi and V. de Giorgio, Phys. Rev. A **3**, 1108 (1971).
[11] D. Meltzer and L. Mandel, Phys. Rev. Lett. **25**, 1151 (1970).
[12] A. Valle, L. Pesquera, and M. A. Rodriguez, Phys. Rev. A **45**, 5243 (1992).
[13] S. Balle, P. Colet, and M. San Miguel, Phys. Rev. A **43**, 498 (1991).
[14] P. Spano, A. Mecozzi, and A. Sapia, Phys. Rev. Lett. **64**, 3003 (1990); A. Mecozzi, P. Spano, and A. Sapia, Opt. Lett. **15**, 1067 (1990).
[15] F. de Pasquale, P. Tartaglia, and P. Tombesi, Physica **99A**, 581 (1979); Phys. Rev. A **25**, 466 (1982).
[16] A. Mecozzi, A. Sapia, P. Spano, and G. P. Agrawal, IEEE J. Quantum Electron. **27**, 332 (1991).
[17] M. M. Choy, P. L. Lui, and S. Sasaki, Appl. Phys. Lett. **52**, 1762 (1988).
[18] S. Singh, Phys. Rep. **108**, 217 (1984).
[19] The numerical simulations have been performed following the algorithm described in J. M. Sancho, M. San Miguel, S. L. Katz, and J. D. Gunton, Phys. Rev. A **26**, 1589 (1982). Typical averages were taken over 5×10^4 realizations using a step of integration of 2×10^{-4}.
[20] M. Suzuki, Adv. Chem. Phys. **46**, 195 (1981).
[21] M. M. Tehrani and L. Mandel, Phys. Rev. A **17**, 677 (1978).
[22] *Handbook of Mathematical Functions*, edited by M. Abramowitz and I. Stegun (Dover, New York, 1970).